Mining, Metallurgy & Exploration (2023) 40:543–553
https://doi.org/10.1007/s42461-023-00740-2

Implications of Shale Gas Well Integrity Failure Near a Longwall Mine Under Shallow Cover

K. M. Ajayi[1] · Z. Khademian[1] · S. J. Schatzel[1] · E. N. Rubinstein[1]

Received: 4 November 2022 / Accepted: 7 February 2023 / Published online: 15 February 2023

Abstract
This study simulates the impact of a shale gas well casing breach near a longwall mine. Field studies are conducted to measure mining-induced permeability changes over the abutment pillar of a longwall mine, and a geomechanical model is developed in 3DEC, a three-dimensional numerical modeling code, to predict the aperture of fractures in the overburden at the study site. The predicted aperture values are used to determine mining-induced permeabilities and the results are compared with the field measurements. These aperture values are provided as inputs into fracture flow code (FFC), which generates a stochastic discrete fracture network (DFN) model for the study site and predicts the potential shale gas flow to the mine. Results from 100 DFN realizations are statistically analyzed using the bootstrapping method to compensate for notable variation in fracture geometry. The results show a significant difference between the gas inflow for nearby panels due to increase in the induced permeability during mining of the second panel. The average gas flow to the mine was calculated as 4.72×10^{-2} m^3/s (49 cfm) for a hypothetical breach at the Sewickley horizon during the first panel mining, 8.97×10^{-3} m^3/s (19 cfm) for a hypothetical breach at the Uniontown horizon during the first panel mining, 2.16×10^{-1} m^3/s (458 cfm) for a hypothetical breach at the Sewickley horizon during the second panel mining, and 8.07×10^{-2} m^3/s (171 cfm) for a hypothetical breach at the Uniontown horizon during the second panel mining. Depending on the mine ventilation system, this could result in methane concentrations exceeding regulatory limits. Hence, these findings provide insights into the potential risk of an unconventional gas well casing breach near a longwall mine under shallow cover.

Keywords Shale gas well · Longwall mine · Shallow cover

1 Introduction

The numbers of unconventional shale gas wells near current or potential future longwall coal mines have increased in the USA due to technology advances in the gas extraction of tight gas deposits. For example, within 1 week in February 2021, the Pennsylvania Department of Environmental Protection (PA DEP) received 19 unconventional gas well permit requests [1]. In some of the locations in Southwestern Pennsylvania, the wells have penetrated different coal seams such as the Sewickley, Pittsburgh, Upper Freeport, and Kittanning seams, which could be mined through within the next few years. The gas pressures from these wells are significantly greater than those from the conventional gas wells, and there could be multiple wells on a single well pad [2]. Any casing breach on this well pad could allow flow of high-pressured gas towards the mine creating safety concerns. Fluid transport in the overburden strata of a longwall mine is dependent on the complex interaction between longwall caving and subsidence, pore pressure, and permeability changes, which are governed by site-specific hydrogeological, geological, and geotechnical conditions [3].

For permeability changes, longwall mining induces stress changes along with surface and subsurface subsidence in the overburden, classified as the caved zone, fractured zone, and continuous zone [4]. The caved zone is characterized by broken rocks and could extend up to 4–6 times the mining height. The fractured zone consists of three parts: rock blocks, vertical fractures, and horizontal fractures due to bedding plane separation as shown in Fig. 1. The lower portion of the fractured zone has three parts; the middle portion has fewer vertical fractures, and the upper part is mainly

✉ K. M. Ajayi
ony2@cdc.gov

[1] Centers for Disease Control and Prevention, National Institute for Occupational Safety and Health, Pittsburgh, PA, USA

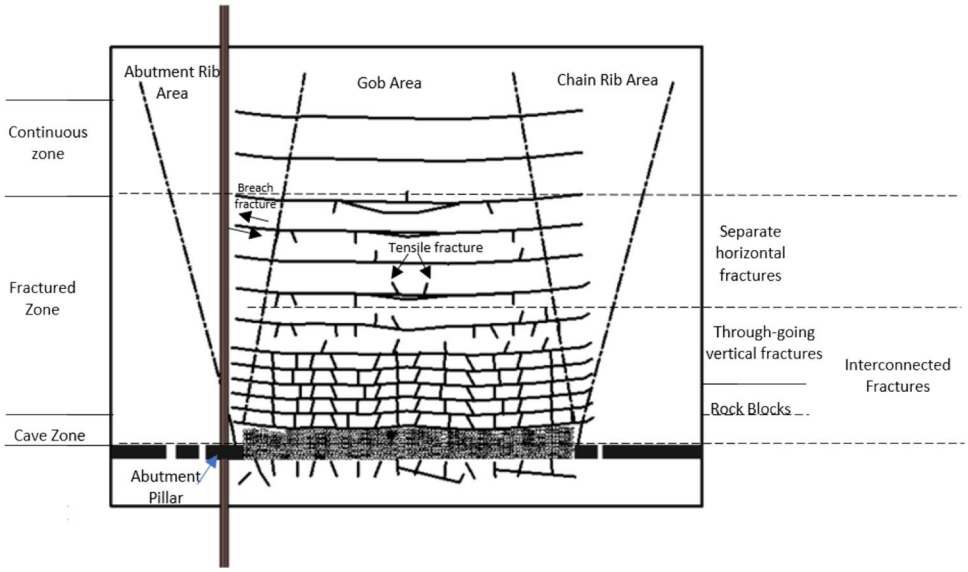

Fig. 1 Illustration of a longwall mine overburden

made up of separate horizontal fractures due to bedding plane separation [5]. This fracture network provides pathway for gas transport through the overburden due mining-induced permeability. Adhikary and Guo measured pre- and post-mining permeability and reported about a 1000-fold increase in permeability over the gob and up to a 50-fold permeability increase in the solid coal pillar [6]. Overtime, it has been proven that numerical models calibrated with field measurements provides are representative of the longwall induced deformation [3].

Similarly, it is important to predict the location of possible casing damage due to mining-induced deformations. The longwall mine data from PA DEP show that the Pittsburgh Coal Seam could range from 73 m (240 ft) to 366 m (1200 ft) below surface. For example, Blacksville mine is mining the Pittsburgh Coal Seam between 192 m (630 ft) and 366 m (1200 ft), and Emerald mine is mining the Pittsburgh Coal Seam between 183 m (600 ft) and 308 m (1010 ft). Similarly, the shale reserves often targeted in these regions are the Marcellus shale, which could have a depth range of 2100 m (7000 ft) to 2750 m (9000 ft). So, it is certain that the gas wells drilled near these mines would penetrate the Pittsburgh Coal Seam. The 2017 technical guidance document highlighted subsidence, pillar deformation, and floor failure as mechanisms that could adversely impact unconventional gas wells [2]. Considering these failure mechanisms, a previous study on this project focused on identifying the potential breach locations at a study site in southwestern Pennsylvania [7]. Inclinometer readings were used to monitor surface subsidence during mining of the first and second longwall panel. The modeling conducted with FLAC3D™ identified the Sewickley and Uniontown Coal Seam horizons as primary zones of horizontal displacement. Horizontal displacements of 17 cm and 4 cm were observed at the Sewickley horizon and at the Uniontown horizon, respectively [7]. To determine the likelihood of gas flow through these horizons, Watkins et al. monitored permeability changes during the mining of two adjacent panels [8]. Therefore, these identified horizons are simulated in this study to predict potential shale gas flow to the mine. The findings in this paper provide insights into an emerging field with limited studies in the literature [9–13].

2 Research Approach

Figure 2 presents an overview of the research approach used in this study. Field studies are conducted to estimate mining-induced permeability at a site mining the Pittsburgh coal seam at 146.9 m (482 ft) horizon. The study conducted slug test over the abutment pillar with three boreholes (FEB1, FEB2, and FEB3 in Fig. 3). A detailed methodology of the field findings is published in [8] and the key findings are presented in Table 1. The fourth borehole (GCB) as shown in Fig. 3 measured ground movement data at the site, which are used for calibration and validation of the geomechanical model.

The geomechanical study was conducted in 3DEC and used to determine aperture of mining-induced fractures from surface to the mine horizon. After validating the geomechanical analysis with the ground movement data, the aperture data are used to model permeabilities and compare them with field measurements at the three specific horizons. The complete descriptions of the geomechanical model along with calibration and validation have been published in [14]. Figure 4 shows the histograms of fracture aperture obtained from 3DEC for horizons near the mine and below the Sewickley horizon. Aperture

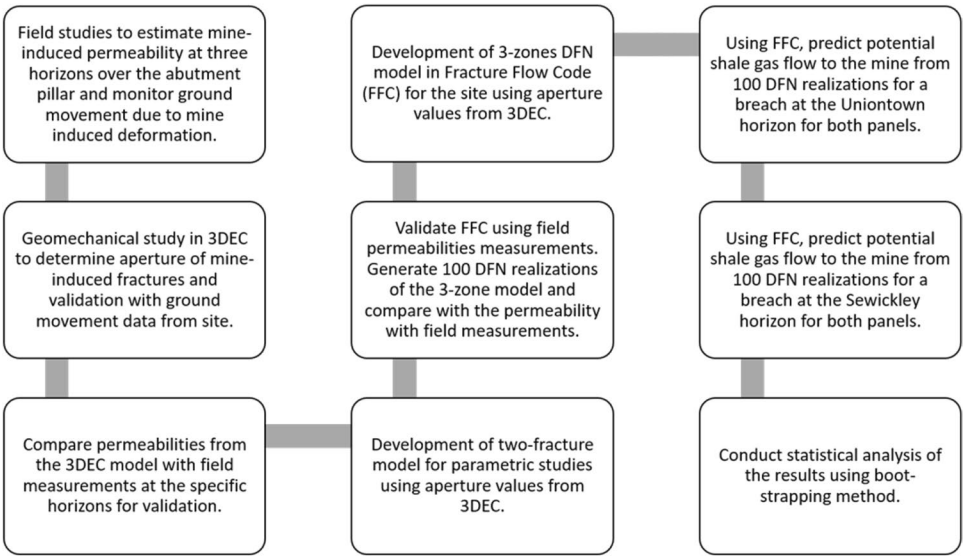

Fig. 2 Summary of research approach used in this study

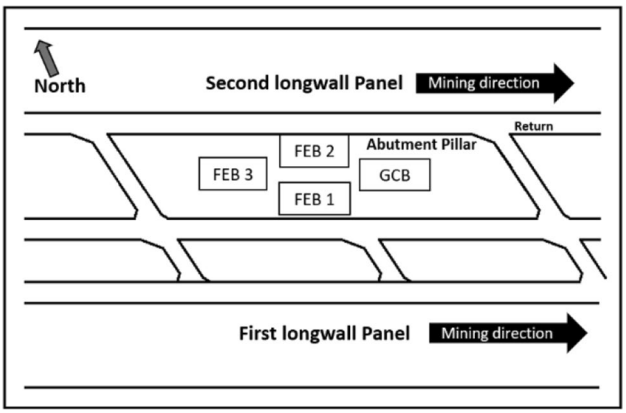

Fig. 3 View of the study site with boreholes used for permeability measurement

values above 1 mm are mostly related to fractures located close to the panel edge where strata curvature and bending occur because of a high concentration of shear and tensile stresses, which activates nearby fractures and enhances their apertures. The smaller values of aperture are associated with the fractures above the gob at the center of the panels. With successful validation of the 3DEC model, the aperture data are used to characterize the gas flow models using fracture flow code (FFC), a code developed specifically for this study. The first flow model consists of two fractures used to study a simplified flow pathway to the mine and predict the isolated impact of pillar setback distance, while the second model is a stochastic discrete fracture network (DFN) model of two longwall panels developed for the study site. Before conducting the comprehensive stochastic analyses using FFC, the code is verified by comparing the results with a similar simplified model developed in 3DEC. After verification, 100 DFN realizations are generated in FFC and simulated to predict gas flow. The results are analyzed using the bootstrapping method for statistical inference from the model.

2.1 FFC Calculations

As illustrated in Fig. 1, fractures are the main conduit for potential shale gas flow to the mine. Therefore, this study develops a discrete fracture network (DFN) method to simulate the impact of the potential casing breach. The DFN approach is often preferred to equivalent continuum model (ECM) because the fractures are modeled explicitly [15]. The model assumes that fracture permeability are orders of magnitude greater than the permeability of the rock matrix. A discrete fracture network (DFN) flow through the fractures is solved using cubic law as follows:

Table 1 Overview of field permeability measurements [8]

Borehole ID	Depth, m (ft)	First panel permeability, m^2 (mD)	Second panel permeability, m^2 (mD)
FEB 1	124.97 (410-ft)	4.07×10^{-13} (411)–1.35×10^{-12} (1,360)	1.09×10^{-12} (1,100)–5.03×10^{-12} (5,080)
FEB 2	79.29 (260-ft)	2.17×10^{-14} (21.9)–2.43×10^{-13} (245)	1.14×10^{-14} (11.5)–3.82×10^{-13} (386)
FEB 3	41.15 (135-ft)	2.70×10^{-12} (2,730)–3.26×10^{-11} (32,900)	3.81×10^{-11} (38,500)–1.31×10^{-10} (132,000)

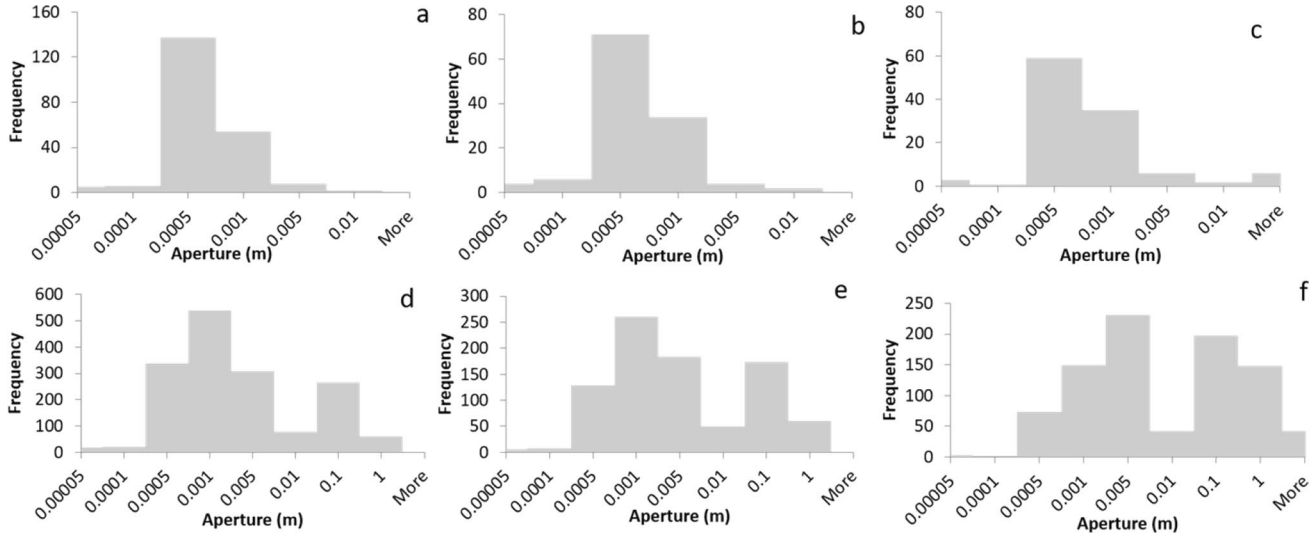

Fig. 4 Aperture of panel 2 vertical fractures: **a** abutment pillar 126.2–128.9 m depth, **b** abutment pillar 128.9–130.7 m depth, **c** abutment pillar 130.7–135 m depth, **d** Gob 126.2–128.9 m depth, **e** Gob 128.9–130.7 m depth, **f** Gob 130.7–135 m depth

$$Q = -\frac{\rho g\, b^3\, w}{12\,\mu\, L}\,\Delta H. \tag{1}$$

In Eq. 1, w is the fracture height. Q is the volumetric flow rate (m^3/s), ΔH is the pressure head difference, μ is the dynamic viscosity of the fluid ($N \bullet s/m^2$), ρ is the density of fluid (kg/m^3), L is the length of the fractures (m), b is the fracture aperture (m), and g is the acceleration due to gravity (m/s^2). As a case study, Fig. 5 shows a simple fracture network with a horizontal and near-vertical fracture. The internal node pressure heads are unknown and are obtained by solving for mass conservation at each of the internal nodes. In this case, it is assumed that the breach occurs at point 1 and the released gas flows through a horizontal fracture to point 2, which is assumed to be the edge of the panel. From point 2, the gas flows through a near-vertical fracture to the mine (point 3). If the gas pressure head at point 3 is zero ($H_3 = 0$) , mass conservation is applied at point 2 and the gas flow to the mine (Q_{23}) is derived as:

$$Q_{23} = \frac{\rho g b_{12}^3 b_{23}^3 H_1}{12\mu \left[b_{12}^3 L_{23} + b_{23}^3 L_{12}\right]}. \tag{2}$$

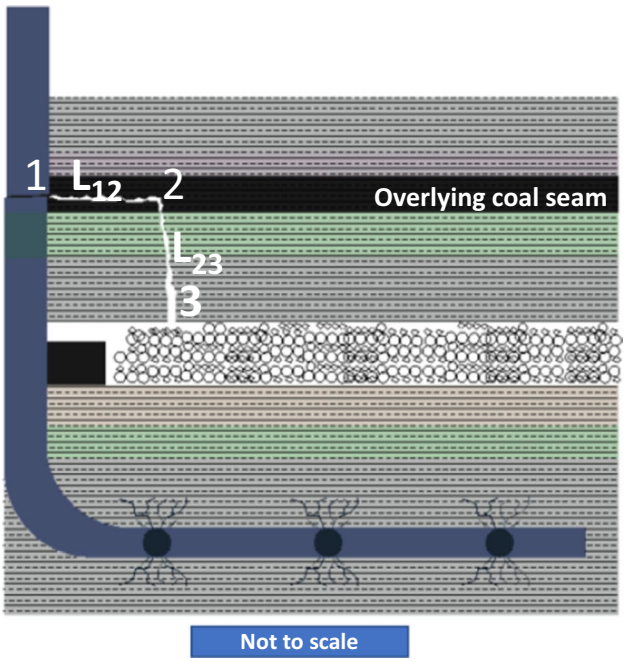

Fig. 5 Schematic of the two-fracture flow model

In Eq. 2, b_{12} is the aperture from points 1 to 2 and b_{23} is the aperture from points 2 to 3. Similarly, L_{12} is the fracture length from points 1 to 2 and L_{23} is the fracture length from points 2 to 3. Q_{23} is the gas flow rate from points 2 to 3. For the stochastic DFN model, FFC uses the same approach by applying mass conservation at the internal node to predict the gas pressure at different locations in the overburden. To illustrate this beyond the two-fracture model in Fig. 5, Fig. 6 shows a deterministic DFN model with 6 internal and 10 external nodes with a hypothetical casing breach at node 15. The pressure at point 15 is defined with pressure of the shale gas and the pressure of the other external nodes are defined as zero. The pressure heads for the internal nodes are obtained by solving the system of equations obtained after

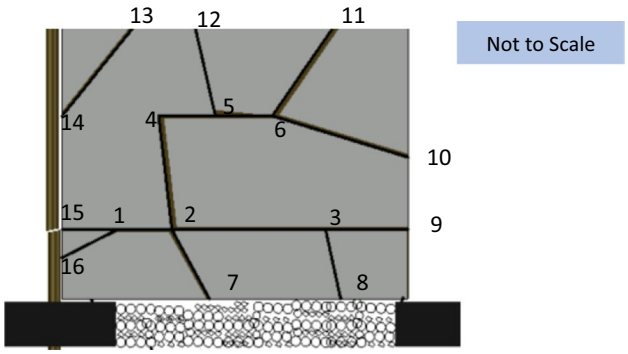

Fig. 6 Illustration of a deterministic DFN model

applying mass conservation at each of the internal nodes. For gas flow from fracture node i, to node j, the volume flow rate in Eq. 1 is represented as:

$$Q_{i-j} = C_{i-j}\left(H_j - H_i\right) \tag{3}$$

where C_{i-j}, the fracture conductance is:

$$C_{i-j} = \frac{\rho g\, b_{i-j}^3\, w}{12\,\mu\, L_{i-j}} \tag{4}$$

By applying mass conservation at the internal node 1, Eq. 5 is obtained:

$$C_{15-1}\left(H_{15} - H_1\right) + C_{16-1}\left(H_{16} - H_1\right) + C_{2-1}\left(H_2 - H_1\right) = 0 \tag{5}$$

This process is repeated for all the internal nodes and a system of equation is obtained and solved in FFC to obtain the internal pressure heads. After obtaining the internal pressure heads, the gas flow across all the boundaries can be calculated since the external pressure heads are assumed to be known [16].

2.2 Stochastic Discrete Fracture Network Model

The potential flow pathways in the overburden could be more complex than the two-fracture case study described in section 2.1. Therefore, this section describes the development of a two-panel DFN model for the site. This model is developed using a FFC developed specifically for this study. The code generates the discrete fracture network and solves for flow based on the defined boundary conditions. Like the geomechanical model, the DFN model is developed based on the site core log data. The overburden strata are classified into 50 layers with thicknesses greater than 0.6 m from the surface (continuous zone) to the top of the caved zone at a depth of 135.3 m (444 ft). The orientations of the near-vertical fractures are modeled with Von-Mises Fisher's distribution [17]. The fracture density is varied to replicate the possible variation in the number of induced fractures from the mine roof to the surface [14]. The aperture of the fractures is modeled with a lognormal distribution proven to be representative of fracture apertures under different stress conditions. Based on the distinct fracture characteristics for fractures over the abutment pillar compared to the gob, each panel is classified into three zones as shown in Fig. 7. The zones over the pillars are classified as rib area (tailgate abutment pillar area and headgate chain pillar area) for each panel. Similarly, the zone over the region where coal has been extracted is classified as the gob area. Therefore, the peak of the lognormal distribution is

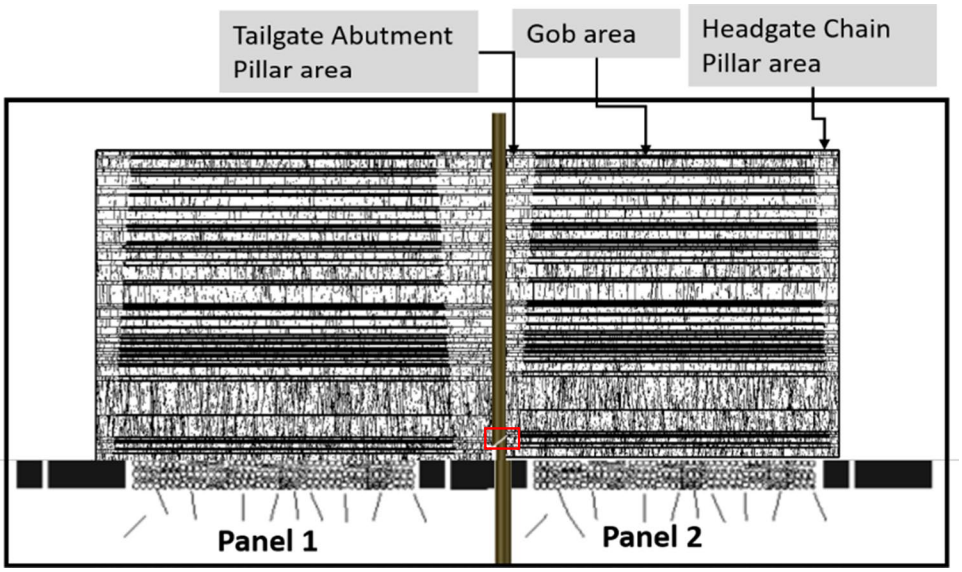

Fig. 7 Stochastic DFN model for panels 1 and 2 with an illustration of a complete casing breach around the Sewickley horizon

selected from the geomechanical studies to predict fracture aperture for different depths.

2.3 Model Validation for FFC

Since the FFC was developed specifically for this study, it is important to verify that the results are representative of field conditions. Therefore, 100 DFN realizations are developed in the FFC and used to predict the permeability changes over the abutment pillar at the Uniontown horizon for the first panel. The permeabilities are then compared with the field measurements as published in [8, 18]. Figure 8 shows the comparison between the measured permeabilities and permeabilities predicted from the FFC for the Uniontown and Sewickley horizon. The results show that each of the DFN realizations is representative of different field conditions. The measured permeability was changing based on the location of the longwall face compared to the measurement location. However, the stochastic DFN approach does not consider the location of the longwall face and time, but the results in Fig. 8 show that this calibrated FFC model has the capability of replicating the variation observed during the field measurements. Therefore, 100 DFN realizations used to simulate a hypothetical casing breach at the Sewickley and Uniontown coal horizons.

2.4 Model Assumptions/Limitations and Boundary Conditions

The model assumes that the properties of shale gas could be represented with methane. The effect of gas generation at different strata in the overburden is not considered since the objective is to predict the isolated impact of the casing breach. Gas desorption within the rock matrix or gas generation along the fracture length is a conventional problem in coal longwall mining with or without a shale gas casing breach. If the strata are non-gas bearing, this impact is minimized but could be impactful if the strata are gas bearing. However, in this study, cubic law is used to predict the isolated impact of the casing breach. Based on knowledge of water saturation for most fractures in the Northern Appalachian basin [19], the fractures are assumed to be 25% saturated with stationary water. This implies that 75% of the aperture opening is available for gas flow—a conservative scenario since the water saturation level could be significantly greater. The predicted gas flow will be higher if the fractures completely drained (dry) and a simulation of the

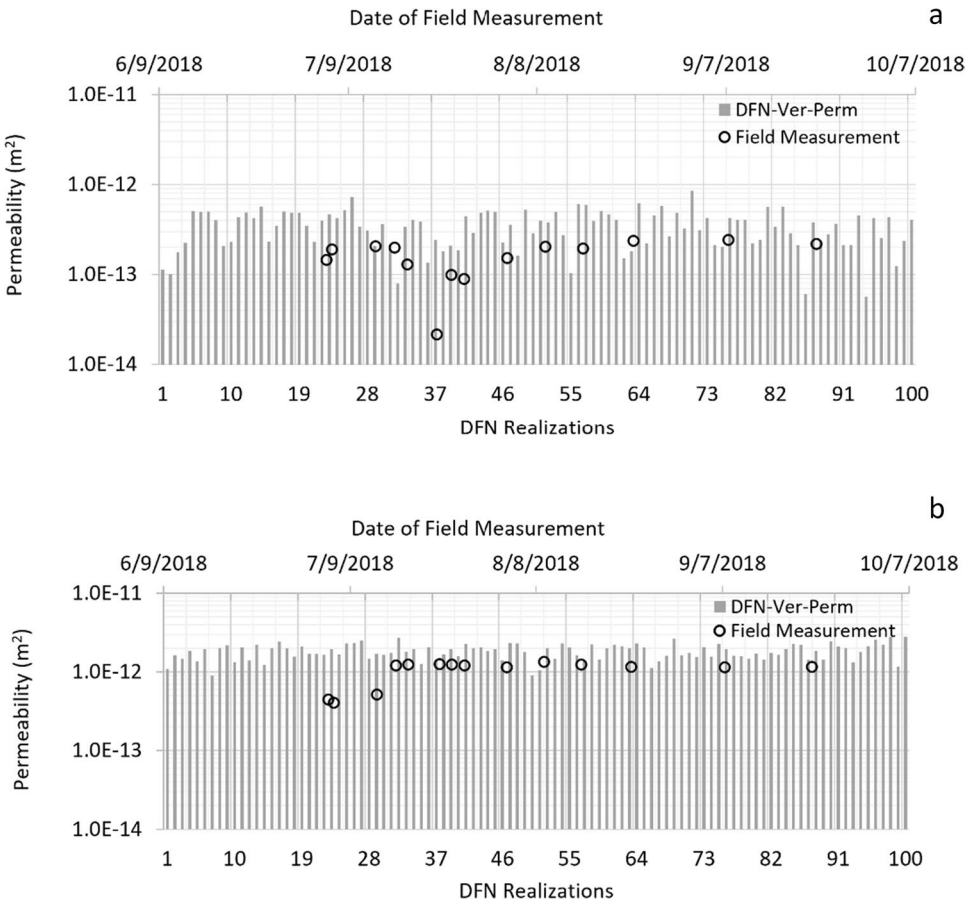

Fig. 8 Comparison of field permeability measurements with permeabilities from 100 DFN realizations during mining of the first panel at the **a** Uniontown horizon and **b** Sewickley horizon

impact of water saturation on the predicted gas flow will be worthwhile for future studies. However, there was water in the boreholes at these horizons over the abutment pillar during the monitoring period and therefore, some level of water saturation is assumed. In the modeling of gas flow in coal mines by Kissell and Edwards's [19], they assumed an initial water saturation of 70% for modeling gas flow in coal mines. It is also possible that fractures over the gob have lower water saturation due to higher permeability and this could be further investigated.

The hypothetical shale gas well casing failure is modeled independently at the two horizons predicted as potential breach locations (Sewickley and Uniontown horizons) [7]. At each horizon, it is assumed that the breach point is at the bedding interface (horizontal fracture) near the casing. Hence, the gas pressure at the horizon is modeled as the pressure of the flowing gas well and is assumed to be 2.41 *MPa* (350 *psi*) and defined at the breach location. Even though some of the gas pressure might be lost as the gas flows into the horizontal fracture, this assumption is made to represent the worst-case scenario, where the horizontal fracture at the breach location is directly connected to the casing. So, the entire 1-m depth of this two-dimensional model is assumed as the source; if the aperture at the breach horizon is 1×10^{-4} *m*, the pressure is applied directly to an area of 1×10^{-4} m^2. For this aperture value, the critical pressure to obtain a 2300 Reynold's number is ≈25.5 *MPa* (3698 *psi*) for a fracture length of 5 m. The gas pressure used in this study is quite representative of the production pressure at this gas sites. However, if the gas well is shut-in, the pressure will be significantly higher.

2.5 Results and Discussion

2.5.1 Gas Flow to the Mine from the Two-Fractures Model

For the case study with two fractures in Fig. 5, Fig. 9 shows the shale gas volumetric flow rate to the mine for different setback distances and fracture apertures in the event of a breach at the Sewickley horizon. This study is conducted using the assumptions described in section 2.4 with a 25% stationary water saturation in the fractures. The setback distance is defined as the length of the horizontal fracture from the breach location to the vertical fracture (L_{12}). To quantify the variation in the gas flow model, the apertures in Fig. 9 are varied in increments of 10%. Figure 9 shows that the gas flow rate increases with an increase in the fracture aperture. Though this is an expected result, the model provides insight into the quantification of the gas flow variation. For the three setback distances and aperture range considered, a 10% increase in the apertures corresponded to over a 20% increase in the gas flow and up to a 33% increase in some

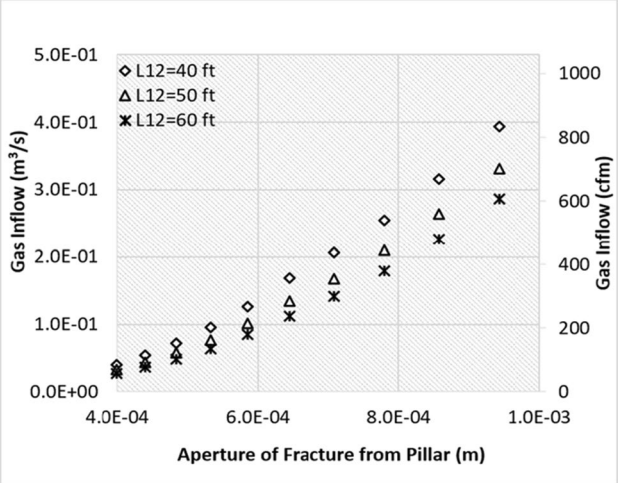

Fig. 9 Results from the two-fracture flow model

cases, which explains the sensitivity of the gas flow to the fracture apertures.

Therefore, a slight increase in the aperture due to mine-induced deformation could change gas flow significantly. Three setback distances: 12.19 m (40 ft), 15.24 m (50 ft), and 18.29 m (60 ft) are considered to study the impact of the shale gas location from the edge of the panel. As shown in Fig. 9, the gas volumetric flow rate is lower for greater setback distances. Even though increasing the setback distance could have some impact on the mine-induced fracture apertures, this study focuses on determining the isolated impact of the setback distance or fracture length on the gas flow rate. With a 25% increase in setback distance from 40 to 50 ft, the gas flow rate decreased by 15–20% depending on the aperture values. Similarly, with a 20% increase in setback distance from 50 to 60 ft, the gas flow rate to the mine decreased by 13–17%. Therefore, using this simple case study, the impact of the setback distance and fracture aperture could be significant for the gas flow to the mine. Consequently, it is necessary to conduct further geomechanical studies on the aperture distribution variation for different setback distances.

2.5.2 Gas Flow from the Stochastic DFN Model

This section discusses the results for 100 DFN realizations generated for mining the first and second panels using the FFC. The choice of 100 realizations for this Monte Carlo simulation assumes that one realization represents 1% likelihood of the fracture network in the overburden. The simulation of multiple realizations further represents the variation in fracture geometry in the overburden similar to the variation observed in the permeability measurements by Watkins

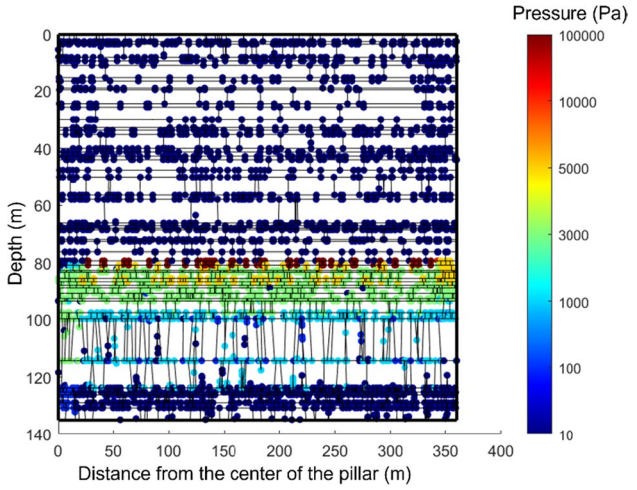

Fig. 10 Gauge pressure distribution for a breach at the Uniontown horizon for one DFN realization

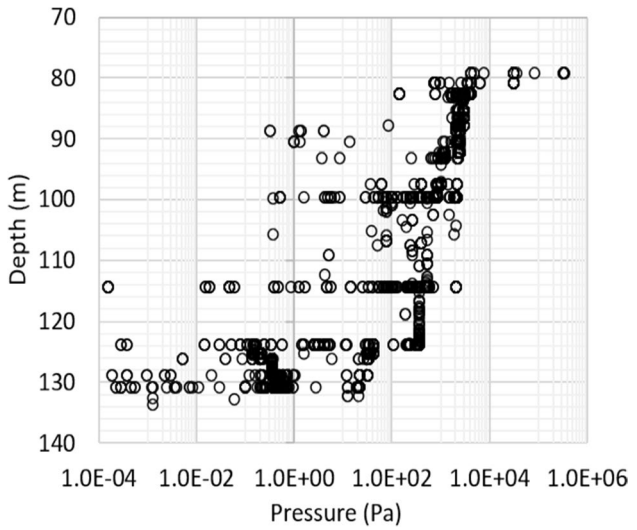

Fig. 11 Gauge pressure plot for a breach at the Uniontown horizon for one DFN realization

et al. [8]. A casing structural failure or breach is modeled at the Sewickley and Uniontown horizons for mining the first and second longwall panels. For a breach at any of the horizons, a pressure loss is anticipated as the gas flows through the nearly closed fractures over the abutment pillar. So, as a case study, Figs. 10 and 11 show a typical gas gauge pressure distribution for a breach at the Uniontown horizon without considering the impact of mine roof pressure. Figure 10 shows a detailed map of the gas pressure from the hypothetical breach point (79 m) to the overburden. Due to the limitation in the range of values that could be displayed in the color map in Fig. 10, Fig. 11 presents the pressure plot with depth to show the exact values near the mine roof. The result shows a significant pressure loss as the gas flows through the underlying strata. At the breach horizon, there are locations where the gas pressure is greater than 100 kPa (14.5 psi) and decreases as it approaches the mine. For this realization, most of the gas flows towards the mine since it is the path of least resistance.

The results from the field measurements show that the mining-induced permeability is greater during completion of the second panel due to the enhanced aperture. Hence, it is anticipated that the impact of a casing breach is greater for the second panel. This model simulates a breach at the Sewickley and Uniontown horizons for both the first and second panels with the summary of results shown in Fig. 12 for 100 DFN realizations. Similar to Fig. 8, there is no time or face position parameter in the plot. However, the realizations with the greatest predicted gas flow have permeabilities in very close range to the maximum field permeability measurement. The results show that the distribution of potential gas flow to the mine is a non-normal distribution for the four conditions simulated. It is further observed that most of the predicted values are within the low ends of the plot (1–400 cfm), which indicates a greater probability that flow to the mine is likely within this low range. The higher ends of histogram are linked to DFN realizations, where the predicted DFN model permeabilities are closest to the greatest values of the experimentally verified permeability, as measured when the longwall face position is close to the well collar or just past it. Obviously, there are notable differences in the inflow based on the breach location and the panel being considered. For both panels, the gas flow to the mine is less for a breach at the Uniontown horizon compared to the Sewickley horizon, which indicates that the risk is lower if the breach location is farther from the mine.

For both horizons, there is a significant difference between the results for the first and second panels due to the differences in the mining-induced permeability. Though these are not absolute values, since the model is two-dimensional, they provide a good measure for comparison on the impact of different parameters in the event of a casing breach. It is also important to note that the flow calculated is the total boundary flow per meter, since FFC is a two-dimensional model that assumes a 1-m thickness in the out-of-plane direction (Table 2). Clearly, the risk is lower if the panel is farther from the pillar and if the potential breach location is farther from the mine and if a bridge layer is present between the mine and the casing breach horizon. These findings provide some relevant information on measures to be used in developing guidelines to ensure safety in similar mines.

2.5.3 Statistical Analysis Using Bootstrapping Method

The motivation for employing an inferential statistical technique was to make probability statements about the 90th

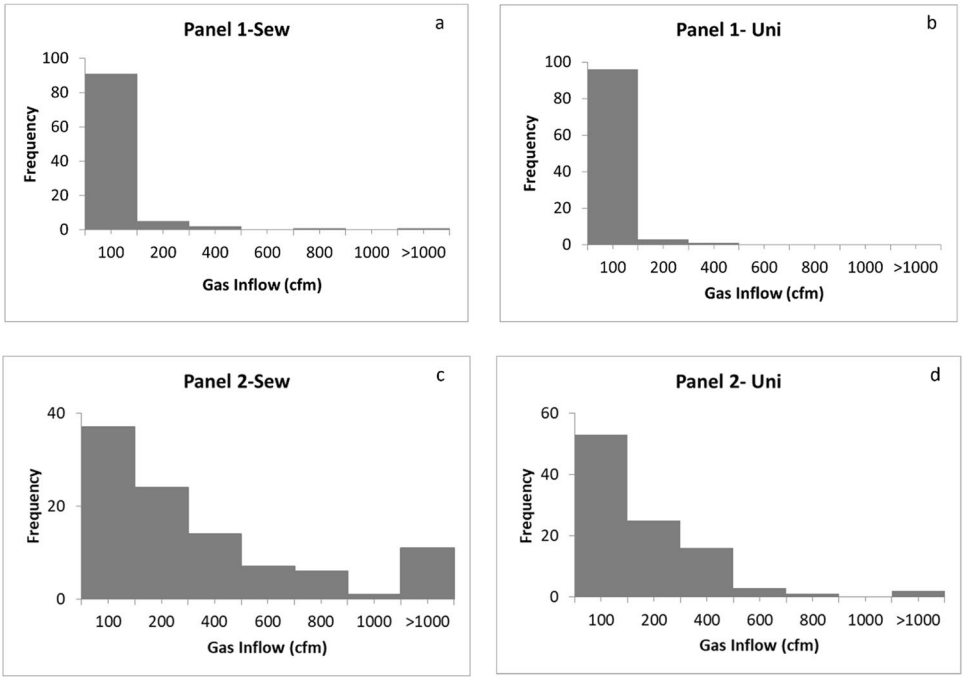

Fig. 12 Histogram of gas flow to the mine for a breach at **a** Sewickley horizon during first panel mining; **b** Uniontown horizon during first panel mining; **c** Sewickley horizon during second panel mining; and **d** Uniontown horizon during second panel mining

Table 2 Average flow to the mine from the simulation of 100 DFN model realizations

	Sewickley horizon	Uniontown horizon
Panel 1	49 cfm	19 cfm
Panel 2	458 cfm	171 cfm

percentile (value marking off the greatest ten percent) of potential gas inflow values. Estimating this parameter allows a description of the range within which the lowest 90% of potential gas inflow values could be expected to fall. If it were reasonable to assume that the distribution of potential gas inflow values could be well approximated by a known theoretical distribution such as the normal distribution, parametric methods (which are based on the assumption of normality) could be used to estimate the percentiles of interest. However, in this case, this assumption would not be reasonable because the distribution of the percentiles of interest in the samples of 100 realizations for the four locations was extremely skewed to the right as shown in Fig. 12. In a right-skewed distribution, most observations are found at the lower end of the range, while relatively few extreme values are found at the upper end of the range. Bootstrapping is a nonparametric procedure, meaning that no assumptions are made about the form of the distribution of the parameter of interest. To estimate the parameter of interest, bootstrapping makes use of the technique of resampling. Resampling involves generating a large number—usually 1000 or more—subsamples or replications from the sample of observed values to approximate the distribution

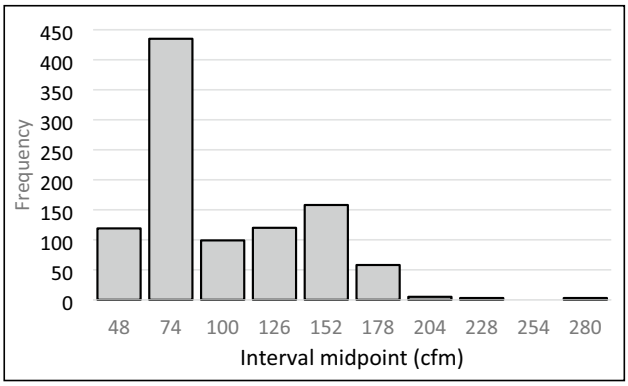

Fig. 13 Distribution of the 90th percentile of gas inflow for a breach at the Sewickley horizon

of the parameter of interest. Sampling is done with replacement, meaning that each observation can be selected multiple times [20].

In the present study, 1000 replications were generated for the 100 DFN realizations for a breach at the Sewickley horizon during mining of the first panel. The 90th percentile was computed and recorded for each replication. A histogram of the 90th percentile value, obtained from 1000 bootstrap replications of the samples of 100 realization values for mining the first panel at the Sewickley horizon, is shown in Fig. 13. The histogram illustrates the extreme right skewness of the 90th percentile distribution, which resulted from the extreme right skewness of the original samples of 100 realizations. For this case study, the mean of the 90th percentile is 100 cfm. *The intent of this section is to establish the*

bootstrapping method as a means of further analyzing the result from the stochastic DFN model and it is verified using one of the case studies. The choice of the Sewickley horizon for this study is because it is closer to the mine compared to the Uniontown horizon. The 90th percentile for the other scenarios is 47 cfm for panel 1 at the Uniontown horizon, 342 cfm for panel 2 at the Uniontown horizon, and 1194 cfm for panel 2 at the Sewickley horizon. Hence, it is prudent to use the 90th percentile to evaluate the impact on the mine ventilation system. Therefore, it is recommended that these values should be incorporated in the mine ventilation model to determine measures for ensuring the safety of the workers in the event of such an occurrence. Further analysis could be conducted using computational fluid dynamics (CFD) to predict specific mine locations where the gas could accumulate. Continuous gas sampling and analysis would be required to proactively predict the presence of shale gas in specific locations of the mine.

3 Conclusions

In this paper, the authors studied an intricate problem by combining field measurements and numerical modeling using a researcher-developed code (FFC) and a commercial software (3DEC). The geomechanical model in 3DEC is used to predict the aperture of the mine-induced fractures, and the gas flow to the mine is simulated using FFC. Though this could be a transient flow problem in real life with several variables, the authors used a steady-state flow assumption to predict potential gas flow to the mine if there is a hypothetical casing breach. The stochastic DFN modeling approach is used to consider the effects of variabilities in fracture length, location, orientation, connectivity, and aperture on the inflow results. The results show that:

a. The location of the breach has a significant impact on the potential gas flow to the mine. In events where the breach location is notably distant from the mine, the gas pressure from the breached casing could drop significantly between the breached location and adjacent strata.
b. The significant differences between the gas flow rates for a breach during mining of the first and second panels could be attributed to an increase in permeability during mining of the second panel.
c. Due to the nonparametric distribution of the inflow range, the mean of the 90th percentile value, which represents the greatest 10%, could be used to predict the impact of the well breach on the mine ventilation.

Though this model has provided results on potential gas flow to the mine in the event of a hypothetical breach, there are further opportunities for improvement. The mining horizon considered in this study is at 146.9 m (482 ft), which is a shallow cover site with anticipated increased permeability changes due to mining. Under a deep cover scenario, the induced permeability could be significantly lower. Hence, a future study of this scenario will be highly beneficial to the industry. The predicted gas flow is the boundary flow per unit meter (m^3/s-m) based on the 1-m depth assigned to the out-of-plane direction. Hence, it is important to study the impact of the out-of-plane length to obtain the absolute gas volumetric flow rate. In addition, this model assigned a peak value for a range of depths as presented in Table 1; the next phase of this study will incorporate the actual 3DEC aperture data with respect to both axes. It is also important to state that this study addresses the potential consequences of one breached well, but some well pads could contain multiple wells and there could be multiple breaches. Hence, there is a need to simulate corresponding scenarios to predict the impact on the mine. Finally, it is also important to note that well performance changes over time such that the parameters used for this simulation could be different. These variabilities could also be considered in future studies. However, the results from this study provide a basis for future analyses and simulations of this intricate problem.

Disclaimer The findings and conclusions in this paper are those of the authors and do not necessarily represent the official position of the National Institute for Occupational Safety and Health, Centers for Disease Control and Prevention. Mention of any company or product does not constitute endorsement by NIOSH.

Declarations

Conflict of Interest The authors declare no competing interests.

References

1. Pennsylvania Department of Environmental Protection, Office of oil and gas management workload report. 2021.
2. Mark C, Rumbaugh GM (2020) Assessing risks from mining-induced ground movements near gas wells. International Journal of Mining Science and Technology 30(1):11–16
3. Adhikary D, Guo H (2015) Modelling of longwall mining-induced strata permeability change. Rock Mechanics and Rock Engineering 48(1):345–359
4. Palchik V (2005) Localization of mining-induced horizontal fractures along rock layer interfaces in overburden: field measurements and prediction. Environmental Geology 48(1):68–80
5. Palchik V (2003) Formation of fractured zones in overburden due to longwall mining. Environmental Geology 44(1):28–38
6. Adhikary D, Guo H (2014) Measurement of longwall mining induced strata permeability. Geotechnical and Geological Engineering 32(3):617–626
7. Su D, Zhang P, Dougherty H, Van Dyke M, Minoski T, Schatzel S, Gangrade V, Watkins E, Addis J, Hollerich C (2019)

Longwall-induced subsurface deformations and permeability changes—shale gas well casing integrity implication. In: Proceedings of the 38th International Conference on Ground Control in Mining. Society for Mining, Metallurgy & Exploration
8. Watkins E, Karacan CÖ, Gangrade V, Schatzel S (2021) Assessing gas leakage potential into coal mines from shale gas well failures: inference from field determination of strata permeability responses to longwall-induced deformations. Natural Resources Research 30:1–14
9. Su DW (2017) Effects of longwall-induced stress and deformation on the stability and mechanical integrity of shale gas wells drilled through a longwall abutment pillar. International Journal of Mining Science and Technology 27(1):115–120
10. Ajayi KM, Khademian Z, Schatzel SJ (2022) Evaluation of parameters influencing potential gas flow to the mine in the event of a nearby unconventional shale gas well casing breach. Mining, Metallurgy & Exploration 39:1–9
11. Bunch A, Perry CS, Abraham L, Wikoff DS, Tachovsky JA, Hixon JG, Urban J, Harris M, Haws L (2014) Evaluation of impact of shale gas operations in the Barnett Shale region on volatile organic compounds in air and potential human health risks. Science of the Total Environment 468:832–842
12. Davies RJ, Almond S, Ward RS, Jackson RB, Adams C, Worrall F, Herringshaw LG, Gluyas JG, Whitehead MA (2014) Oil and gas wells and their integrity: implications for shale and unconventional resource exploitation. Marine and Petroleum Geology 56:239–254
13. Soeder DJ, Sharma S, Pekney N, Hopkinson L, Dilmore R, Kutchko B, Stewart B, Carter K, Hakala A, Capo R (2014) An approach for assessing engineering risk from shale gas wells in the United States. International Journal of Coal Geology 126:4–19
14. Khademian Z, Ajayi KM, Su DWH, Esterhuizen G, Schatzel SJ (2021) Geomechanical modeling of mining-induced permeability: implications for potential gas inflow from a sheared gas well. In: 40th International Conference on Ground Control in Mining. Canonsburg, PA
15. Hadgu T, Karra S, Kalinina E, Makedonska N, Hyman JD, Klise K, Viswanathan HS, Wang Y (2017) A comparative study of discrete fracture network and equivalent continuum models for simulating flow and transport in the far field of a hypothetical nuclear waste repository in crystalline host rock. Journal of Hydrology 553:59–70
16. Priest SD (2012) Fluid flow in discontinuities, in Discontinuity analysis for rock engineering. Springer Science & Business Media
17. Best D, Fisher NI (1979) Efficient simulation of the von Mises distribution. Applied Statistics 28:152–157
18. Ajayi K, Khademian Z, Schatzel S, Watkins E, Gangrade V (2022) A discrete fracture network model for prediction of longwall-induced permeability. Mining, Metallurgy & Exploration 39:1–8
19. Kissell FN, Edwards JC (1975) Two-phase flow in coalbeds. USBM Report of Investigation 8066
20. Mooney CZ, Duval RD (1993) Bootstrapping: a nonparametric approach to statistical inference. sage 89:1150